PROCEEDINGS, TOUGH Symposium 2006
Lawrence Berkeley National Laboratory, Berkeley, California, May 15–17, 2006

TOUGH+/GasH2O STUDY OF THE EFFECTS OF A HEAT SOURCE BURIED IN THE MARTIAN PERMAFROST

George J. Moridis and Karsten Pruess

Lawrence Berkeley National Laboratory
Berkeley, CA. 94720, USA
E-mail: GJMoridis@lbl.gov

ABSTRACT

We use TOUGH+/GasH2O to study the effects of a heat source buried in the Martian permafrost to evaluate the possibility of establishing a wet zone of liquid water, in which terrestrial microorganisms could survive and multiply. Analysis of the problem indicates that (1) only a limited permafrost volume (not exceeding 0.35 m in radius) is affected, (2) a "wet" zone with limited amounts of liquid water develops (not exceeding 8 and 0.7 kg for a 250 W and a 62.5 W source, respectively), (3) the wet zone persists for a long time, becomes practically stationary after t = 20 sols because of venting into the Martian atmosphere, and its thickness is limited and decreases slowly over time, (4) a "dry" zone (where $S_G > 0.9$) evolves, continues to expand (albeit slowly) with time, but its extent remains limited, and (5) the ice front surrounding the wet zone is self-sharpening. For a range of initial conditions investigated, evolution of the liquid water mass occurs at approximately the same rate, reaches roughly the same maximum, and occurs at about the same time (10 to 20 sols; 1 sol = 24.39 hours).

INTRODUCTION

Background

This study was undertaken as part of the Planetary Protection project of NASA (Vasadava, 2004), which seeks to protect solar planets and their satellites (that are under consideration for possible exploration by rovers) from earth-originating biological contamination. Of particular importance is the protection of Mars, where two solar-powered rovers are already operating, and to which a new generation of rovers may be sent before 2010. Among the primary goals of future missions involving the new generation of rovers will be to investigate the existence of water (in liquid or ice form) and the possibility of life (past or present) on Mars.

The Mars Odyssey Gamma Ray Spectrometer (GRS) Suite has detected large amounts of hydrogen within the top meter of the Martian surface layer poleward of 60° latitude in each hemisphere (and at certain longitudes poleward of 45° latitude), and smaller amounts of hydrogen at lower latitudes (Boynton *et al*., 2002; Mitrofanov *et al*., 2002; Feldman *et al*., 2002). The current interpretation is that ice saturations S_I reach high levels (50-75%) in the subsurface at high latitudes. This Martian permafrost is covered by roughly 10-20 cm of dry regolith. Lower-latitude features indicating presence of water may be due to bound water, adsorbed water, or spatially unresolved patches of ground ice, and correspond to observed water-equivalent hydrogen volume percentages below 12%. Morphological evidence (Head *et al*., 2003) suggests sublimation of an icy surface may have occurred in the 30º-60º latitude band. No such evidence is present for latitudes equatorward of about 30º.

Given the focus of future missions, prospective landing sites for the next generation of Martian rovers are located at high latitudes (60° and above) because of the accumulated evidence that high ice saturations are to be encountered there. Solar-powered generation for these rovers is not feasible because of limited solar radiation at these latitudes and the corresponding need for impractically large solar panels. Radioactivity-based power sources are one alternative under consideration.

Objective

The objective of this study is to determine the effects of a heat source buried in the Martian subsurface and in contact with the Martian permafrost. Such a heat source (powered by radioactivity) can originate from the destruction of the vehicle (rover) upon failure of the landing system (e.g., parachute malfunction).

The focus of this study is the determination of the possibility of the creation of a wet zone of liquid water, in which terrestrial microorganisms that might be carried by the landing vehicle could conceivably survive and multiply. Such microbial populations are assumed to be able to survive the extreme temperature and radiation conditions en route from Earth to Mars. Their ability to survive and multiply would endanger the success of subsequent missions addressing the question of past life on Mars.

Approach

We investigated by means of numerical simulation the effects of a continuous heat source embedded in the Martian soil, using parameters and conditions provided to us by the Jet Propulsion Laboratory (Vasadava, 2004). The investigation included a simplified scoping study (involving a 1D radial system) and a set of large simulations (involving high-definition 2D cylindrical domains) that

realistically described likely scenarios of system behavior in response to the embedded heat sources.

The Numerical Model

For these simulations, we used the TOUGH+/GasH2O numerical code (Moridis et al., 2006), consisting of the TOUGH+ core code with the GasH2O module (describing the equation of state of a system involving a real gas mixture and water). TOUGH+ is the most advanced generation of the TOUGH2 family of codes (Pruess et al., 1999) developed at the Lawrence Berkeley National Laboratory. It is written in FORTRAN 95/2003 to take advantage of the object-oriented capabilities and the enhanced computational features of that language. TOUGH+ employs dynamic memory allocation (thus minimizing storage requirements), follows the tenets of Object-Oriented Programming (OOP), and involves data encapsulation, polymorphism, derived types and classes (defining the various objects), pointers, constructors and destructors, dynamic linkage, inheritance, operator overloading, and interoperability with C/C++ subroutines.

TOUGH+ is based on the Integral Finite Difference Method (Narasimhan and Witherspoon, 1976), and can solve strongly non-linear problems of multiphase fluid flow (by advection, dispersion and diffusion) and heat transport (through advection, conduction and radiation) in complex geologic media by employing the Jacobian and the Newton-Raphson iteration. The basic principles, underlying formulation and numerical implementation are described in Pruess et al. (1999) and Moridis et al. (2005a). The code accurately describes phase changes and the thermophysical properties of fluids of interest (e.g., water and gases) through the entire ice-to-liquid-to-vapor spectrum.

1-D RADIAL SYSTEM STUDY

System Description and Simulation Strategy

As a first step in this study, a simple 1-D radial system of ice in the Martian subsurface was investigated. The domain had a thickness of 1m. A heat source of 250 W was specified in the center of the system. The hydraulic and thermal properties of the porous media listed in Table 1 represent our best current understanding of the shallow Martian subsurface.

The initial pressure P and temperature T were typical of those prevailing on Mars. Because of the lack of data on the relative permeability and capillary pressure of ice-bearing systems, these were assumed to follow the vanGenuchten (1980) model. Additionally, the effect of the solid phase (ice) on the wettability behavior of the Martian subsurface was accounted for by using the Evolving Porous Medium (EPM #2) model (Moridis et al., 2005a;b), which is based on data from solid precipitation in soils.

Table 1. Conditions and Properties in the 1D Study

Parameter	Value
Porous medium	Regolith
Regolith grain density ρ	2800 kg/m^3
Initial P	713 Pa
Initial T (at interface)	–80 ^{o}C
Atmospheric composition	100% CO_2
Permeability k	10^{-13} m^2 (= 0.1 D)
Porosity ϕ	0.50
Initial ice and gas saturations	S_I = 0.3, S_G = 0.7
Heat capacity of medium C	800 J/kg/K
Dry thermal conductivity k_Θ	0.2 W/m/K
Relative permeability and capillary pressure model: Van Genuchten (1980)	λ = 0.6 P_0 = 25000 Pa
Irreducible gas saturation S_{irG}	0.01
Irreducible aqueous phase saturation S_{irA}	0.12
Exponent n of the EPM #2 model (Moridis et al., 2005b)	3

The grid was composed of 200 gridblocks of a uniform radial increment Δr = 0.025 m, followed by 50 logarithmically increasing radial increments that terminated at an outer boundary at r = 200 m. Implicit in the study of this 1-D radial system was the assumption that its upper and lower boundaries were impermeable and insulated (i.e., the system cannot exchange mass and heat with its surroundings). This assumption limits the degrees of freedom of the system, and results in higher P and T.

The main objective of this study was to gain a first insight into the behavior of a system in which we had little prior experience. The 1-D study can identify the important parameters and processes, provide a basic understanding of the expected system response, and allow a sharper focus for more complex multidimensional studies. An additional reason for this simplified study was to test (and increase confidence in) the TOUGH+/GasH2O model, as such systems are known to have similarity solutions with respect to the variable r^2/t (where r is the radius, and t is the time). Thus, if the underlying physics of TOUGH+/GasH2O solutions is correct, the predictions of all the system variables (e.g., P, T, saturations) should coincide when plotted against r^2/t.

Results and Discussion

The results shown in Figures 1 and 2 correspond to an initial S_I = 0.3. When plotting the T distributions (Figure 1) at different times t as functions of r^2/t, the resulting curves coincide, thus confirming the property of similarity solution of the system (O'Sullivan, 1981). This provides confidence in the model predictions. The plot of the liquid water saturation S_W vs.

r^2/t (Figure 2) further confirms the similarity solution. Note that, because of the sharp saturation fronts (as opposed to the smooth T profile in Figure 1) and discretization errors (more pronounced at earlier times), the saturation curves do not coincide initially, but tend toward the same solution as time advances.

The importance of this study is that, by confirming the similarity solution, we obtain a robust tool for the estimation of the upper limit of the liquid water zone (LWZ) evolving in the Martian subsurface. The approach is illustrated in Figure 3, in which the T and S_W profiles (as functions of r^2/t) are superimposed, defining simultaneously the location and extent of the LWZ and the corresponding T range. From Figure 3, it is evident that, for the system conditions and properties of Table 1, the LWZ begins at $(r^2/t)_0$ = 5.78×10^{-9} m^2/s and ends at $(r^2/t)_F$ = 3.83×10^{-8} m^2/s. Thus, at t = 8.862×10^6 sec (=100 sols, a sol being the length of the Martian day), the LWZ begins at r_0 = 0.226 m and ends at r_f = 0.583 m. At t = 8.862×10^7 sec (=1000 sols), r_0 = 0.716 m and r_f = 1.842 m. These results indicate that, under the conditions of the 1-D radial problem (involving heat and fluid exchange only though the outer radial boundary), a substantial (and expanding) LWZ evolves in the Martian subsurface. Figure 3 indicates that water remains liquid up to temperature slightly over 60 ^{o}C. This is made possible by the higher pressures that develop in the vicinity of the heat source as water begins to boil.

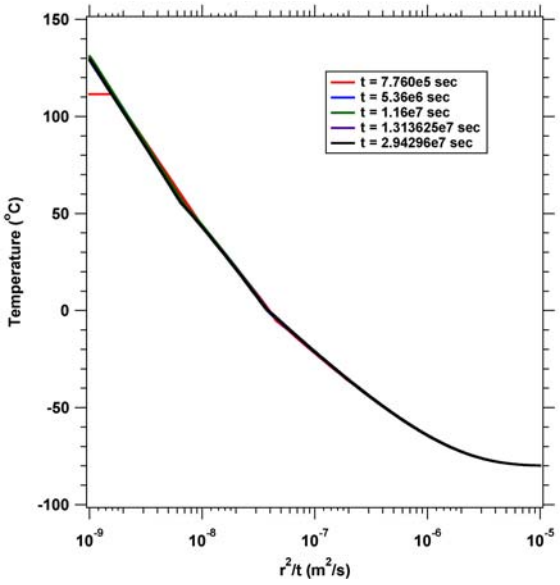

Figure 1. Numerically determined similarity solution of T vs. r^2/t for the 1D radial problem.

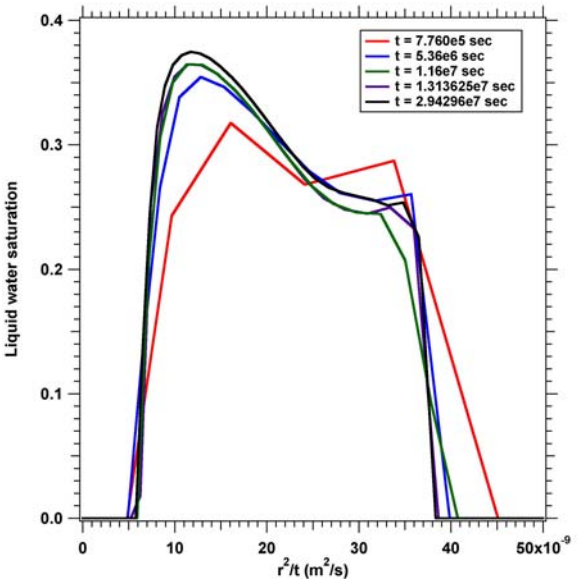

Figure 2. Numerically determined similarity solution of S_W vs. r^2/t for the 1D radial problem.

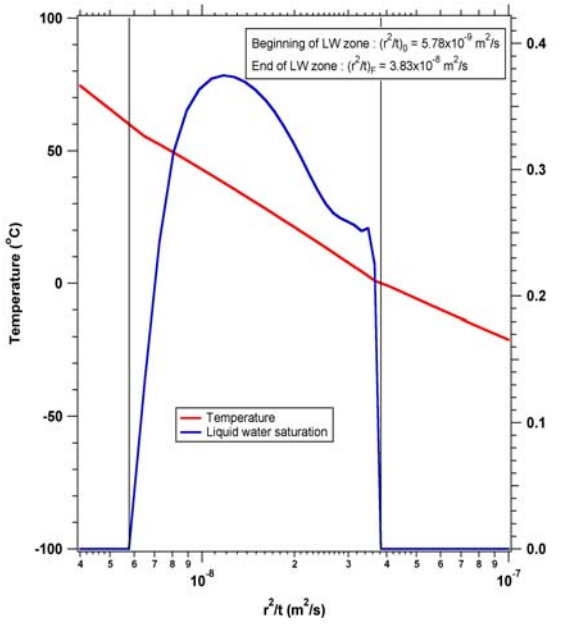

Figure 3. A robust solution of the location and extent of the LWZ for the 1D radial problem.

2-D CYLINDRICAL SYSTEM STUDY

System Description

These studies involved simulations of realistic 2-D cylindrical systems. Based on impact analysis for a wide range of vehicle velocity, the heat source was assumed to be buried under 0.2 m of dry, ice-free Martian topsoil (S_G = 1), and embedded in the top 0.05 m of the Martian permafrost, i.e., from z = -0.2 m to z = -0.25 m (Vasadava, 2004). The hydraulic and thermal properties of the system were as in Table 1. The upper boundary of the system was the Martian atmosphere, kept at a constant P and T (Table 1).

Heat loss to the atmosphere can occur through advection of the escaping fluids, as well as through radiation. To describe radiative heat losses, an emissivity of 0.5 was used. Two heat source strengths were considered: Q_H = 250 W and Q_H = 62.5 W. The heat source was assumed to have the physical and thermal properties of PuO_2, i.e., k_S = 0 m^2, ρ_S= 11400 kg/m^3, C_S = 100 J/kg/K and $k_{\Theta S}$ = 8 W/m/K.

Grid and Simulation Specifics

The grid included three boundary subdomains: (1) a top boundary, representing the Martian atmosphere, (2) a bottom boundary of constant pressure and temperature, and (3) an outer radial boundary of constant pressure and temperature. We used fine discretization in the vicinity of the buried source. Thus, based on earlier scoping studies, the first 50 radial increments were uniform in size with Δr = 0.01 m. An additional 62 radial increments increased progressively from Δr = 0.02 m to 0.2 m and terminated at an outer boundary where r_{max} = 20 m. In the vertical direction, of the 106 layers used to discretize the 16.5-m depth, those that corresponded to the region of maximum expected change near the heat source had a uniform thickness of Δz = 0.01 m, while those closer to the boundaries had a coarser discretization. The domain discretization resulted in 11,440 active gridblocks.

Case 1: Q_H = 250 W Case

The source was cylindrical with r = 0.10 m and a height h = 0.05 m. Starting with the likely S_I = 0.50 as a reference, we varied S_I between 0.10 and 0.95 to determine the sensitivity of system response to the presently unknown S_I in the Martian permafrost.

Cumulative System Response. Figure 4 shows the evolution of the total mass of liquid water (LW) in the 2D cylindrical study discussed above. Figures 5 and 6 show the corresponding vapor and heat flow rates (losses) into the Martian atmosphere. The main conclusions that can be drawn from these figures are the following:

(1) Despite significantly different initial S_I, the evolution of LW begins at about the same time, occurs at similar rates, follows the same pattern, and reaches a similar maximum in the various S_I cases. This observation indicates that the system is (a) remarkably insensitive to significant variability in its initial ice conditions, and (b) uniform in its response. Its insensitivity is attributed to the proximity of the Martian atmosphere to the top of the permafrost (0.2 m), resulting in fast vapor advection and venting to the Martian atmosphere (Figure 5) in addition to rapid radiative heat losses (Figure 6).

(2) From a practical standpoint, the maximum LW mass for any S_I appears small (ranging between 5 and 8 kg), and occurs very early in all cases (between 5 and 20 sols), after which point it decreases slowly and persists for a long time.

(3) For S_I > 0.35, the maximum LW mass increases with a decreasing initial S_I. This is because a lower S_I results in a lower k_Θ (because ice is a strong heat conductor) in addition to increased composite heat capacity C_C of the soil + liquid water + ice system (in which case, heat is expended to raise the temperature of the larger amount of ice).

(4) For S_I < 0.35, the maximum LW mass decreases with a decreasing S_I because of reduced ice availability, which outweighs the effects of k_Θ and C_C.

(5) The dependence of vapor fluxes to the atmosphere on the S_I (Figure 5) mirrors that of the LW on S_I for the reasons discussed in items (3) and (4).

(6) Heat losses to the Martian atmosphere increase with a decreasing S_I because the corresponding lower k_Θ and C_C lead to larger localized temperatures and, consequently, to larger radiative losses.

Spatial Distributions. In the analysis of the spatial distributions, we use the reference case of S_I = 0.5. The evolution of the liquid water saturation S_W distribution in Figure 7 indicates that the *wet zone* (i.e., a zone of LW) is very limited in extent, and does not extend beyond r = 0.35 m, z = -0.50 m at any time. The outer boundary of the wet zone becomes practically stationary after t = 20 sols because of boiling, vapor venting and heat losses into the Martian atmosphere. The thickness of the wet zone is limited (<0.07 m), and decreases slowly over time.

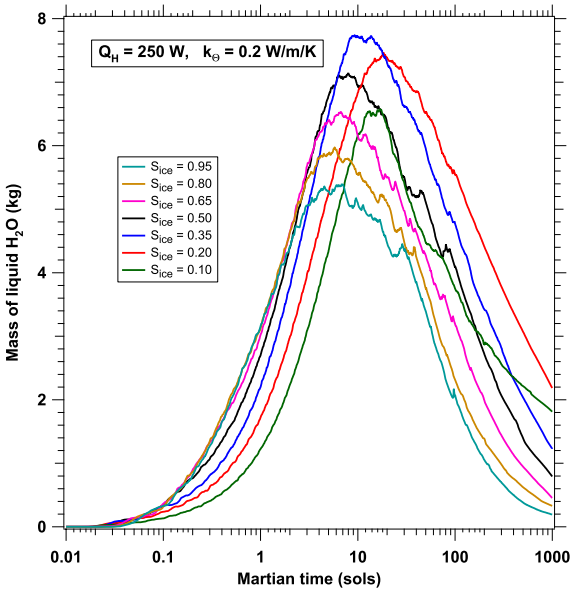

Figure 4. Dependence of the total LW mass on S_I in the 2D study of Case 1.

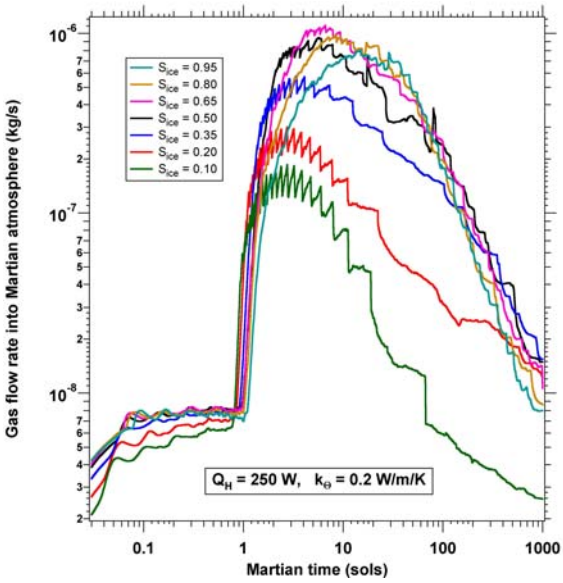

Figure 5. Dependence of gas flux into the Martian atmosphere on S_I in the 2D study of Case 1.

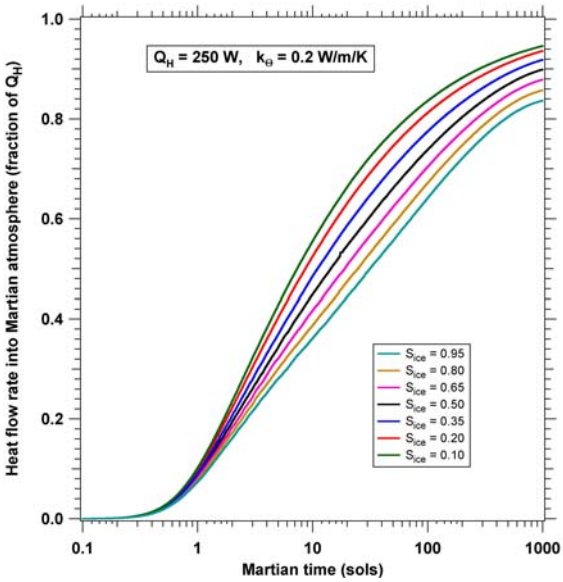

Figure 6. Dependence of heat flux into the Martian atmosphere on S_I in the 2D study of Case 1.

The gas saturation S_G distributions in Figure 8 indicate the evolution of a *dry zone* (defined as the region where $S_G > 0.9$), the inner surface of which continues to expand (albeit slowly) as time advances (while the outer appears stationary). The extent of the dry zone is limited, and does not reach beyond r = 0.30 m, z = -0.50 m after 1000 sols. The dry zone creates a high-permeability region that allows fast vapor flow and venting from the boiling wet zone to the Martian atmosphere. The evolution of the ice saturation S_I distribution in Figure 9 provides an additional explanation for the limited extent and stationary nature of the outer boundaries of the wet and dry zones. The very high (and increasing with time) S_I saturations (resulting as water at the outer boundary of the wet zone forms secondary ice) create an ice barrier that does not allow liquid water or vapor flow through its mass, but redirects flow towards the Martian atmosphere. This observation is further supported by the evolution of the pressure distribution in Figure 10, which provides evidence of fast vapor venting into the Martian atmosphere (in a direction perpendicular to the isobars). Figure 10 indicates boiling along the liquid-gas interface, which appears more intense in the lower parts of the disturbed zone.

Finally, review of the temperature distributions in Figure 11 indicates that the warm zone (defined as the region where T > 0 ^oC, where LW is possible) expands as time advances, but very slowly after t = 100 sols. This is expected in light of the very significant heat losses (Figure 6) and the reliance on the slow process of conduction to raise the temperature in the subsurface. The extent of the "warm" zone is limited, and does not reach beyond r = 0.35 m, z = -0.55 m after 1000 sols. Very steep gradients are observed (evidence of the low conductivity in the dry zone), but these do not lead to an extended warm zone.

Case 2: Q_H = 62.5 W Case

In this case, the source was cylindrical with r = 0.05 m and a height h = 0.05 m. As in Case 1, we varied S_I between 0.10 and 0.95 to determine the sensitivity of system response to the presently unknown S_I in the Martian subsurface.

Cumulative System Response. Figure 12 shows the evolution of the total mass of liquid water (LW) in the Q_H = 62.5 W study. Figure 13 shows the corresponding heat flow rates (losses) into the Martian atmosphere. The results are entirely analogous to those observed in Case 1. The evolution of LW begins at about the same time for practically all S_I levels and follows the same development pattern, thus indicating the system insensitivity to significant variability in the S_I. Compared to Case 1, the maximum mass of LW is about an order smaller (ranging between 0.15 and 0.65 kg), and is attained early in all cases (between 1 and 10 sols). For reasons already discussed, the maximum LW mass and heat losses to the Martian atmosphere increase consistently with a decreasing initial S_I.

Spatial Distribution. The S_W distribution in Figure 14 indicates that the *wet zone* (i.e., a zone of LW) is significantly smaller than the one in Case 1 (extending to r < 0.15 m and z > -0.35 m), and becomes discontinuous much earlier because of the weaker source and the continuous vapor venting and heat flux into the Martian atmosphere.

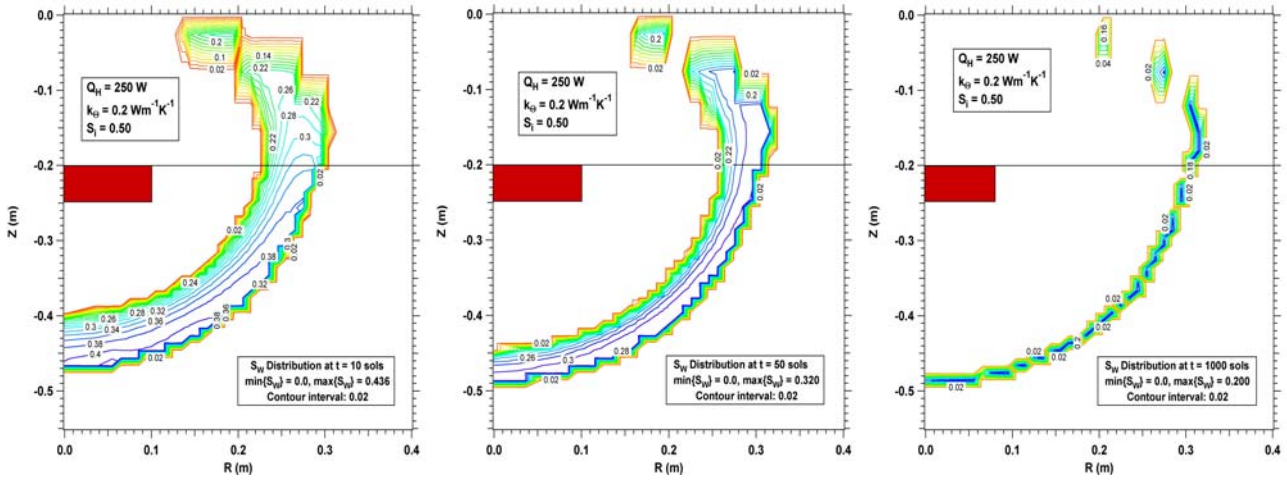

Figure 7. Case 1: Evolution of the water saturation (S_W) distribution over time and development of the wet zone.

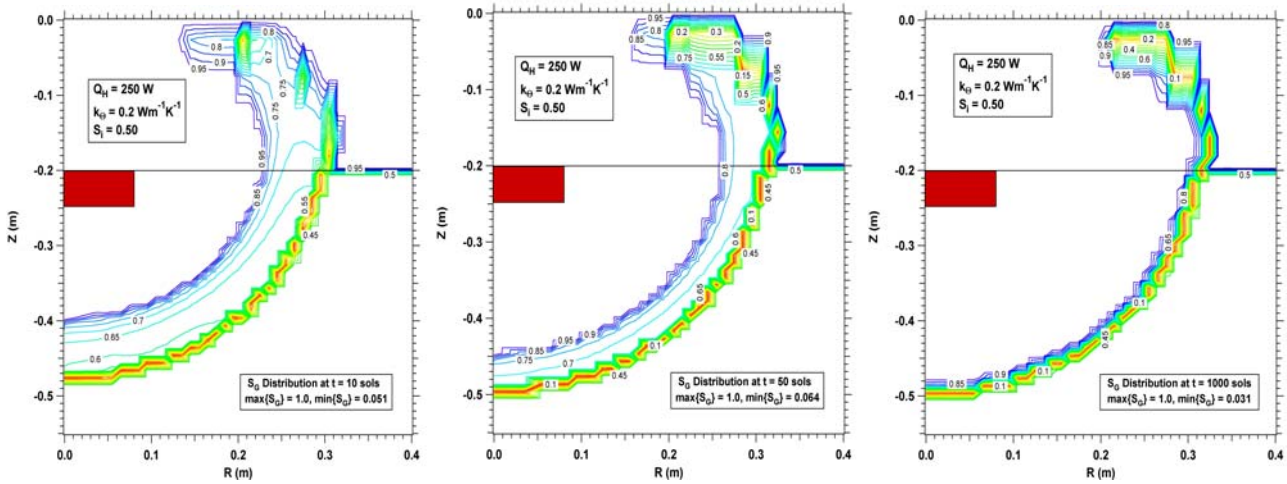

Figure 8. Case 1: Evolution of the gas saturation (S_G) distribution over time and development of the dry zone.

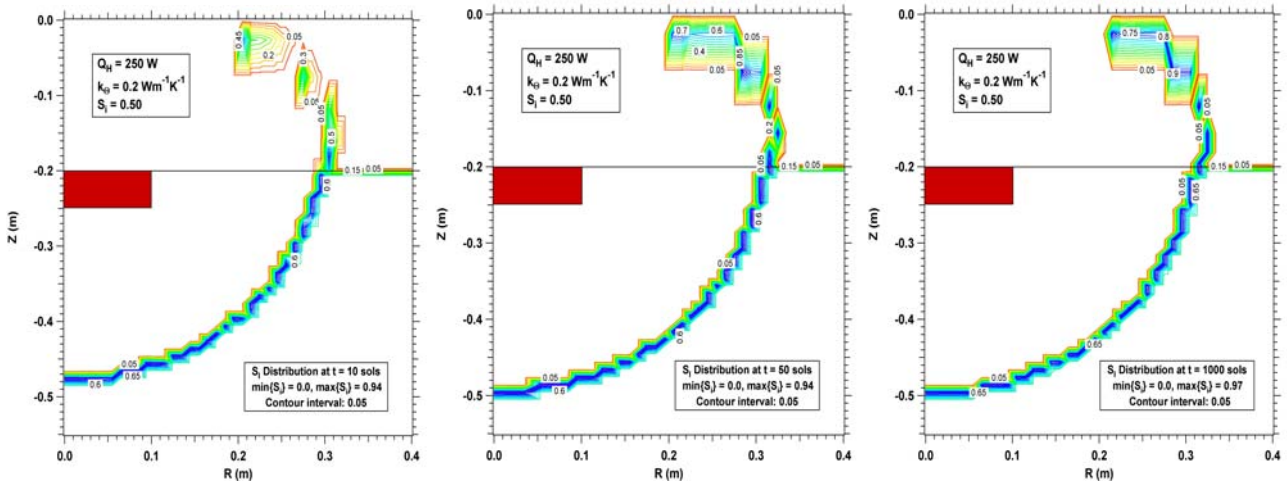

Figure 9. Case 1: Evolution of the ice saturation (S_I) distribution over time and development of the ice barrier.

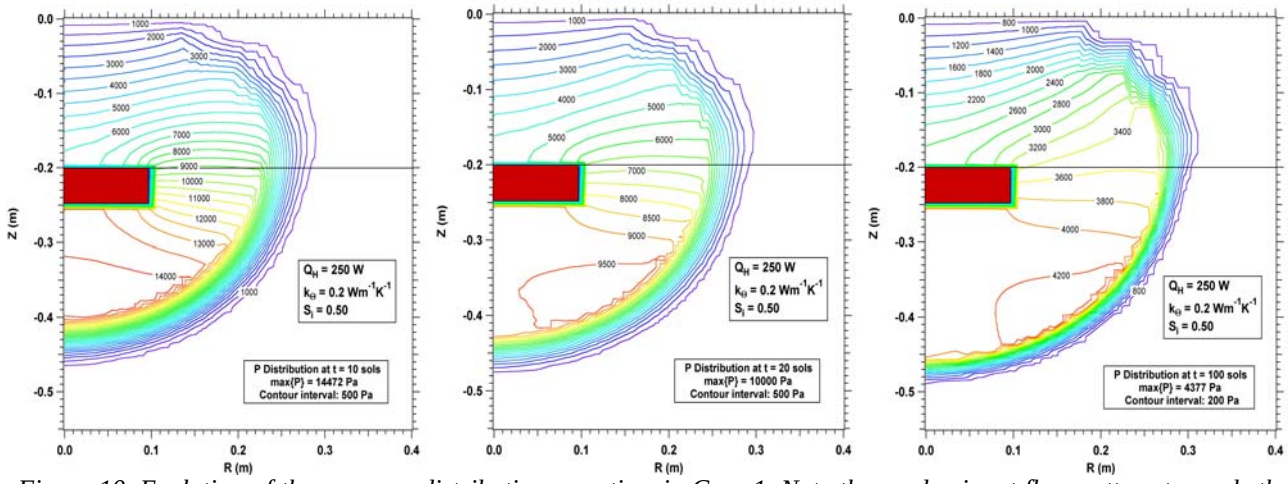

Figure 10. Evolution of the pressure distribution over time in Case 1. Note the predominant flow pattern towards the Martian atmosphere (perpendicular to the isobars).

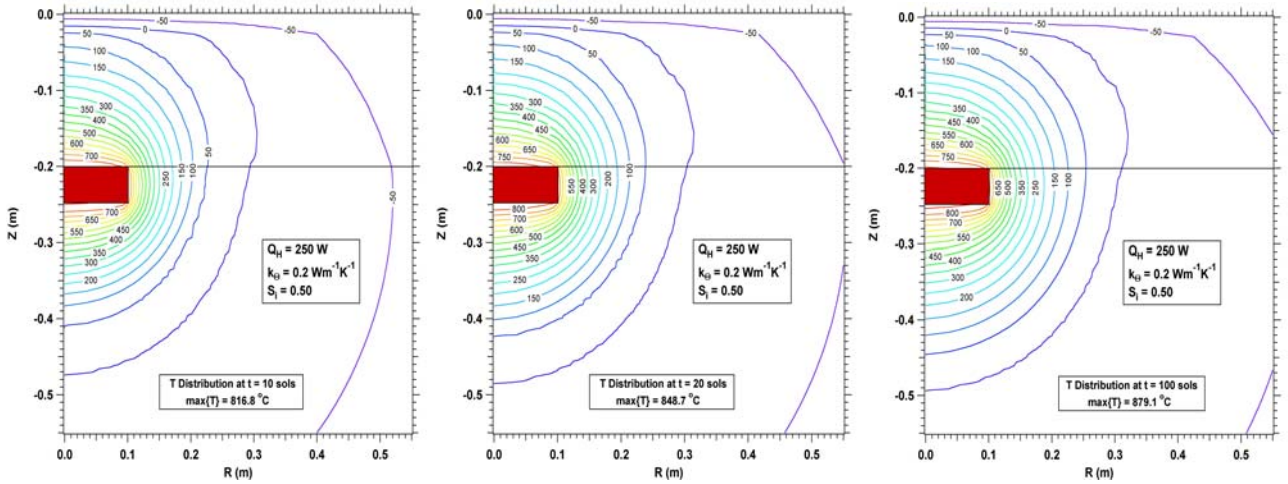

Figure 11. Evolution of the temperature distribution over time in Case 1. Note the steep gradients near the source.

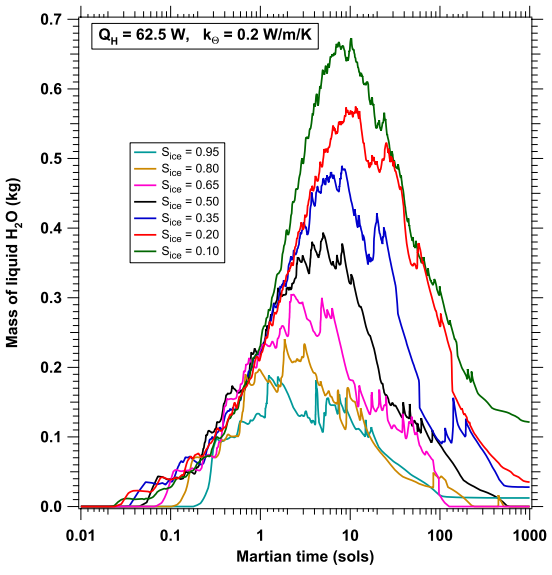

Figure 12. Dependence of the total LW mass on S_I in the 2D study in Case 2.

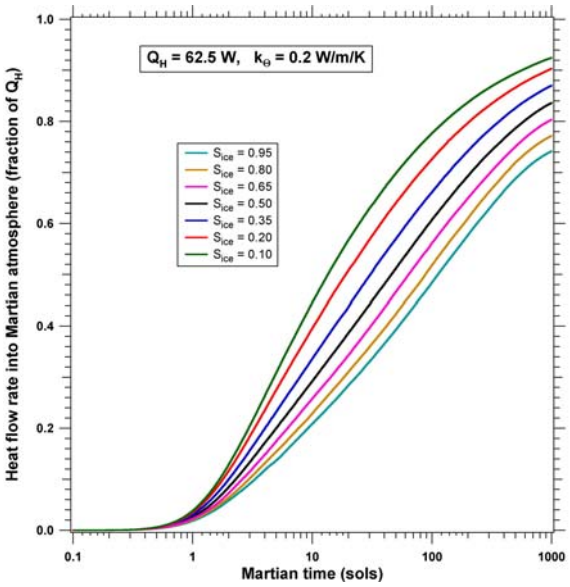

Figure 13. Dependence of heat flow rate into the Martian atmosphere on S_I in the 2D study in Case 2.

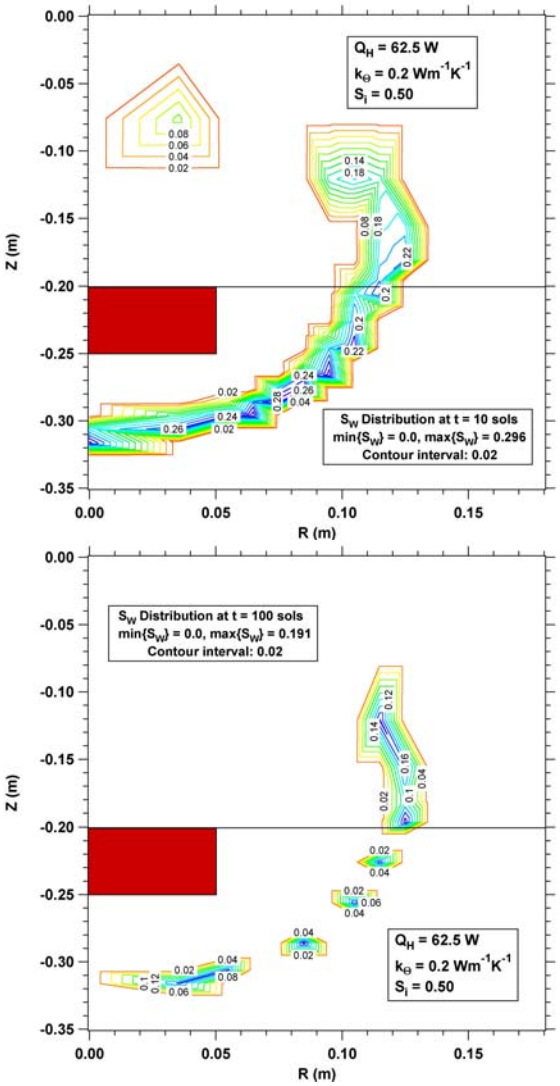

Figure 14. Case 2: S_W distribution at t = 10 and t =100 sols, showing the smaller extent of the wet zone and its discontinuous nature at later times.

SUMMARY

1. TOUGH-Fx/GasH2O can accurately capture the similarity solution of an advancing melting ice front in a simplified 1D radial study of heating of the Martian permafrost.
2. For a given heat source strength, significantly different initial ice saturation S_I lead to LW mass evolution that begins at about the same time, occurs at similar rates, and reaches maximum levels that are not very different. This is attributed to fast vapor and heat loss into the Martian atmosphere.
3. The maximum LW mass in all cases is observed very early, i.e., between 1 and 20 sols.
4. Generally, the maximum attainable LW mass increases with a decreasing initial S_I because of lower composite k_Θ and C. At higher Q_H levels, the opposite may occur at S_I < 0.35 because of limited ice availability.
5. Compared to Case 1 (Q_H = 250 W), the maximum LW mass in Case 2 (Q_H = 62.5 W) is about an order of magnitude lower.
6. The disturbed zones (*dry*, *wet* and *warm*) in the Martian permafrost are very limited in extent, change very slowly after about 100 sols, and can persist for up to 1,000 sols or more.

ACKNOWLEDGEMENTS

This work was supported by NASA through the Jet Propulsion Laboratory, through contract No. DE-AC02-05CH11231 with the U.S. Department of Energy. The authors are indebted to Matt Reagan, John Apps and Dan Hawkes for their thorough review.

REFERENCES

Boynton, W.V. et al., Distribution of hydrogen in the near surface of Mars: Evidence for subsurface ice deposits, *Science*, 297(5578): 81-85, 2002.

Feldman, W.C. et al., Global distribution of neutrons from Mars: Results from Mars Odyssey, *Science*, 297(5578): 75-78, 2002.

Head, J.W., J.F. Mustard, M.A. Kreslavsky, R.E. Milliken, and D.R. Marchand, Recent ice ages on Mars, *Nature*, 426: 797-802, 2002.

Mitrofanov, I. et al., Maps of subsurface hydrogen from the High Energy Neutron Detector, Mars Odyssey, *Science*, 297(5578): 78-81, 2002.

Moridis, G.J., M.B. Kowalsky, S. Finsterle, and K. Pruess, *TOUGH+: The New Generation of Object-Oriented family of Codes for the Soluation of Problems of Flow and Transport in the Subsurface*, LBNL Report number pending, paper presented at the TOUGH Symposium 2006, Berkeley, CA, May 15-17, 2006.

Moridis, G.J., Kowalsky, M.B., and K. Pruess, *TOUGH-Fx/HYDRATE v1.0 User's Manual: A Code for the Simulation of System Behavior in Hydrate-Bearing Geologic Media*, Report LBNL-58950, Lawrence Berkeley National Lab., Berkeley, CA, 2005a.

Moridis, G.J., M.B. Kowalsky, and K. Pruess, *Depressurization-Induced Gas Production From Class 1 Hydrate Deposits*, SPE 97266, 2005 SPE Annual Technical Conference and Exhibition, Dallas, Texas, U.S.A., 9 – 12 October 2005b.

Narasimhan, T.N., and P.A. Witherspoon, An integrated Finite Difference method for analyzing fluid flow in porous media, *Water Resour. Res.*, 12(1): 57–64, 1976.

O'Sullivan, M.J., A similarity method for geothermal well test analysis, *Water Resour. Res.*, 17(2): 390-398, 1981.

Pruess, K., C. Oldenburg, and G. Moridis, *TOUGH2 User's Guide – Version 2.0*, Report LBL-43134, Lawrence Berkeley Laboratory, Berkeley, CA 1999.

van Genuchten, M. Th., A closed-form equation for predicting the hydraulic conductivity of unsaturated soils, *Soil Sci. Soc. Am. J.*, 44: 892-898, 1980.

Vasadava, A., *Mars Surface Characteristics and Models*, Presentation to LBNL and Private Communication, June 2004.